

Structural evolution of FeCO₃ through decarbonation at elevated temperatures

J Wang¹, T Sakakura¹, N Ishizawa^{1,3} and H Eba²

¹ Ceramics Research Laboratory, Nagoya Institute of Technology, Asahigaoka, Tajimi, Gifu 507-0071, Japan

² Tokyo City University, Tamazutsumi, Setagaya-Ku, Tokyo 158-8557, Japan

E-mail: ishizawa@nitech.ac.jp

Abstract. The structural evolution of siderite (s), FeCO₃, through decarbonation at elevated temperatures has been investigated by the *in-situ* single-crystal X-ray diffraction technique using an area detector. When the crystal was heated above 255 °C, the transparent crystal turned colour in faint black from surface, indicating that the decarbonation commenced. The spinel-type magnetite (m), Fe₃O₄, first appeared in coexistence with the FeCO₃ parent crystal. The orientation relationship between the rhombohedral FeCO₃ and the cubic Fe₃O₄ can be described as [111]_m // [001]_s, and [2-1-1]_m // [120]_s. On further heating, additional diffraction spots appeared at 411 °C. They were indexed on the basis of the corundum-type hematite (h), (α-Fe₂O₃). The rhombohedral α-Fe₂O₃ unit cell had the same orientation relationship with the parent rhombohedral FeCO₃ one, i.e., [001]_h // [001]_s, and [100]_h // [100]_s. On further heating the parent FeCO₃ phase disappeared completely at 464 °C. The formation of iron oxides in FeCO₃ depended on not only temperature but also the holding time. The structural relationships among FeCO₃, Fe₃O₄, and α-Fe₂O₃ are discussed.

1. Introduction

The FeCO₃, siderite (s), is commonly found in hydrothermal veins, and considered as potential CO₂ mineral trapping [1]. A use of Fe/CO₂ fuel cells for CO₂ mitigation has been examined [2]. The decarbonation of the FeCO₃ product is important in a view point of carbon monoxide retrieval as a carbon resource. The thermal decomposition of FeCO₃ has been reviewed [3-5]. Decarbonation of carbonate salt has been considered to occur topotaxially [6-8]. Studies on iron carbonate, however, are quite few [9-10] in spite of its importance in an environmental point of view. The present study was thus undertaken to unveil the evolution of siderite structure associated with the decarbonation.

2. Experimental

Single-crystals of FeCO₃ were grown by the hydrothermal method. A preliminary check about the extinction rules of reflections of the rhombohedral FeCO₃ at the room temperature was carried out at the beamline 14A, Photon Factory, KEK, using a horizontal-type four-circle diffractometer [11]. The *in-situ* X-ray diffraction experiments were carried out at elevated temperatures using a single-crystal CCD diffractometer (Smart Apex II, Bruker) with Mo Kα laboratory source [12]. A crystal was

³ To whom any correspondence should be addressed.

mounted on a silica glass capillary by Sauereisen cement (#970000, Niraco Co.), and soaked in a preheated nitrogen gas stream. The temperature at the crystal position was calibrated by the K-type fine gauge thermocouple (KFC-50-200-100, Anbe SMT Co.).

Intensity distribution in reciprocal space was investigated through the sets of contiguous frame data so that more than 99% of crystallographically-independent reflections within $2\theta < 60^\circ$ can be measured. Each of the frame data was taken by either ω or ϕ scan techniques in the range of 0.3° with each exposure time of 5 s. It took 4-12 hours to collect a set of data at one temperature. The experimental temperatures span from room temperature to 825°C . Integrated intensities were extracted from the frame data. The cell parameters were refined from all the observed reflections in the integration process. The SHELXL least-squares program [12] with WinGX crystallographic program package [13] was used for the structure refinement and the other calculations.

3. Results and discussion

Crystals of FeCO_3 have the rhombohedral $R\text{-}3c$ structure at room temperature. When the crystal was heated above 255°C , the transparent crystal turned color in faint black from surface, indicating that the decarbonation commenced. The reciprocal sections of the diffraction pattern at 359, 411 and 464°C are shown in figure 1. On heating, the spinel-type Fe_3O_4 , magnetite (m), appeared first. The orientation relationship between the rhombohedral FeCO_3 (s) and cubic Fe_3O_4 (m) can be described as $[111]_m // [001]_s$, $[2\text{-}1\text{-}1]_m // [120]_s$, as shown in figure 2.

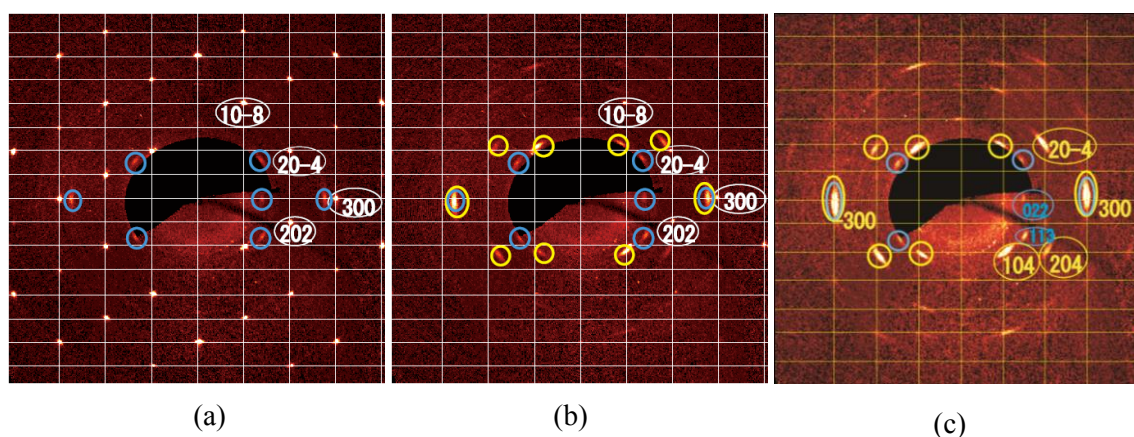


Figure 1 The $(h0l)^*$ sections of the reciprocal space of the FeCO_3 parent phase at 359 (a), 411 (b) and (c) 464°C . Encircled diffraction spots in blue and yellow are spinel-type iron oxide (Fe_3O_4 or $r\text{-Fe}_2\text{O}_3$) and corundum-type $\alpha\text{-Fe}_2\text{O}_3$. The FeCO_3 parent lattice is drawn in white with some indexed spots.

On further heating, additional diffraction spots encircled by yellow color in figure 1(b) appeared at 411°C . They were indexed on the basis of the corundum-type $\alpha\text{-Fe}_2\text{O}_3$, hematite (h). The rhombohedral $\alpha\text{-Fe}_2\text{O}_3$ unit cell had the same orientation relationship with the parent rhombohedral FeCO_3 , i.e., $[001]_h // [001]_s$, $[100]_h // [100]_s$. On further heating the parent FeCO_3 phase disappeared completely at 464°C , as shown in figure 1(c). The diffraction spots of the remaining iron oxides were slightly diffuse, but still showed a toptaxial relationship with the parent siderite lattice. This experiment suggested that the carbon oxide detached from the siderite single crystal, leaving iron oxide components. The formation of iron oxide in FeCO_3 depended on not only temperature but also the holding time. When samples were heated longer than 30 h at some low temperatures like 255°C , for example, the spinel-type Fe_3O_4 was able to form.

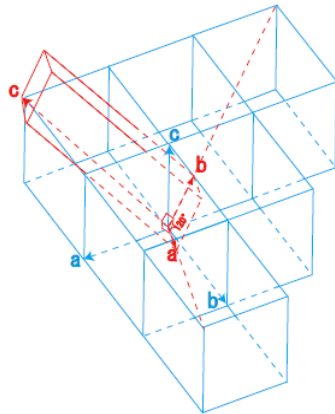


Figure 2. Orientation relationship between FeCO_3 (red) and Fe_3O_4 (blue) unit cells.

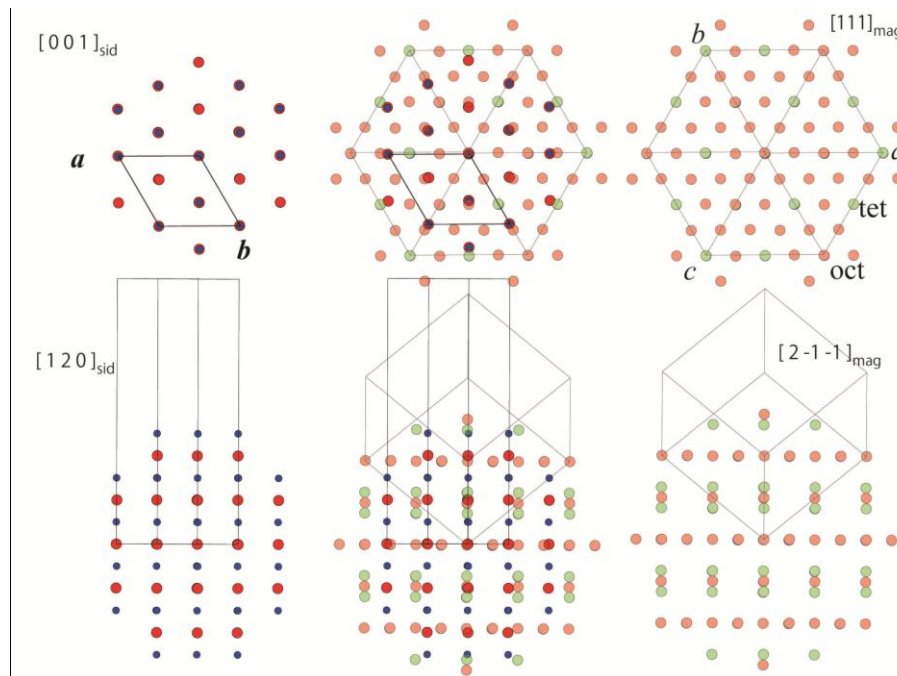


Figure 3. Structures of FeCO_3 viewed along $[001]$ (top-left), Fe_3O_4 along $[111]$ (top-right), and their superposition (top-middle), and structures of FeCO_3 viewed along $[120]$ (bottom-left), Fe_3O_4 along $[2-1-1]$ (bottom-right), and their superposition (bottom-middle),

The orientation relationship between FeCO_3 and spinel-type Fe_3O_4 , as shown in figure 2, can be explained from the structural point of view. The structures of FeCO_3 along $[001]$ and $[120]$, and those of Fe_3O_4 along $[111]$ and $[2-1-1]$ are shown in figure 3. The superpositions of the corresponding pairs drawn in the middle of figure 3 indicated the rationality of the orientation relationships, and accordingly, justified the origin of topotaxy of Fe_3O_4 in the FeCO_3 parent crystal.

The orientation relationship between FeCO_3 and $\alpha\text{-Fe}_2\text{O}_3$ can also be understood from the superposition of the structures along $[001]$, as shown in figure 4. The oxygen packing of FeCO_3 and $\alpha\text{-Fe}_2\text{O}_3$ are essentially the same, whereas the C atoms in FeCO_3 are replaced with Fe in $\alpha\text{-Fe}_2\text{O}_3$.

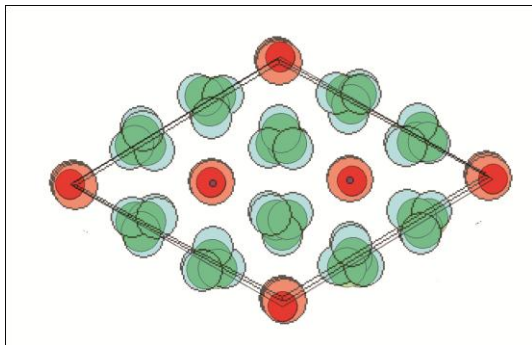


Figure 4. Superposition of FeCO_3 and $\alpha\text{-Fe}_2\text{O}_3$ structures along $[001]$: O (light blue), Fe (orange), and C (blue dot) in FeCO_3 ; O (green), and Fe (red) in $\alpha\text{-Fe}_2\text{O}_3$

Acknowledgements

This work was supported by the Grant-in-Aids for Scientific Research No. 1820671 and No. 22360272 from the Japan Society for the Promotion of Science. Part of the diffraction study was carried out at Photon Factory, KEK, on the basis of the program 2009G005. JW and TS appreciate the research assistant scholarships from the Institute of Ceramics Research and Education, Nagoya Institute of Technology.

References

- [1] James L P, Robert J R, Yousif K K 2005 *Applied Geochemistry* **20** 2038
- [2] Rau G H, 2004 *Energy Conversion and Management* **45** 2143
- [3] Kissinger H E, Mcmurdie H F and Simpson B S 1956 *J. Ameri. Ceram. Soci.* **39** 168
- [4] Gallagher P K and Warren S S J 1981 *Thermochimca Acta* **46** 253
- [5] Heuer J K and Stubbins J F 1999 *Corrosion Science* **41** 1231
- [6] Singh A, Dash S, Kamruddin M, Ajikumar P K, Tyagi A K, Raghunathan V S and Raj B 2002 *J.Am. Ceram. Soc.* **85** 927
- [7] Floquet N and Niepce J C 1977 *J. Mater. Scie.* **12** 1052
- [8] Oh K D, Morikawa H, Iwai S and Akao M 1980 *Ceram. Soc. Japan* **88** 431
- [9] Bernal J D, F R S, Dasgupta D R and Mackay A L 1959 *Clay Mine. Bull.* **4** 15
- [10] Dasgupta D R 1961 *Indian J. Phys.* **35** 401
- [11] Wang J, Sakakura T, Ishizawa N, Eba H 2010 Siderite, FeCO_3 *Photon Factory Activity Report 2008* **28 Part B** in press
- [12] Ishizawa N, Kondo S, Hibino H, Igarashi S, Nakamura M, Saho R 2007 Annual Report of Ceramics Research Laboratory 2006, Nagoya Institute of Technology **6** 12
- [13] Sheldrick G M, 2008 *Acta Cryst.* **A64** 112
- [14] Farrugia L J, J. 1999 *Appl. Cryst.* **32** 837